

Degradation of nitrobenzene by nano-TiO₂ catalyzed ozonation

Yixin Yang, Jun Ma*, Qingdong Qin, Xuedong Zhai

School of Municipal and Environmental Engineering, Harbin Institute of Technology, PO Box 2627, 202 Haihe Road, Harbin 150090, PR China

Received 13 June 2006; received in revised form 5 September 2006; accepted 7 September 2006

Available online 14 September 2006

Abstract

Nano-TiO₂ particles prepared by the sol–gel method were used as catalyst for the degradation of nitrobenzene by ozone. Catalyst samples were characterized by measuring the specific area (S_{BET}), transmission electron microscopy (TEM), and X-ray diffraction (XRD). Removal efficiency of nitrobenzene (NB) was significantly promoted in the presence of catalyst compared with ozone alone. TiO₂ calcined at 500 °C showed the best activity. Different experimental conditions like catalyst dose, ozone dosage, initial nitrobenzene and pH have been examined. The mechanism of catalytic ozonation was also discussed. Both ozonation and catalytic ozonation were significantly influenced by carbonate and *tert*-butyl alcohol, which confirmed that TiO₂-catalyzed ozonation follows a radical-type mechanism. And hydroxyl radicals were truly identified by spin-trapping/EPR technique.

© 2006 Elsevier B.V. All rights reserved.

Keywords: Catalytic ozonation; TiO₂; Ozone; Nitrobenzene; Nanoparticle; Hydroxyl radicals; EPR

1. Introduction

Ozone has been applied to various aspects of water treatments because of its high reactivity with organic compounds. However, it has been reported that in conventional ozonation process most of the organic compounds are not degraded completely by ozone alone and sometimes toxic intermediates are produced. In this case, the oxidation can be improved by employing ozone together with H₂O₂ and/or UV, or in particular, with a solid phase metal oxide catalysts. For example, it was reported that [1] TiO₂-catalyzed ozonation was more efficient for the degradation of humic acid and oxalic acid than ozone alone, furthermore, the increase of the oxidant power of catalytic ozone resulted in low chlorine demand and a reduction of THM formation potential. Subsequent studies were conducted [2] with a solid catalyst prepared by supporting TiO₂ on alumina in the ozonation of drinking water. In this work, high extent of degradation of organic matter was achieved without dissolution of titanium in the water. Consequently, the potentially harmful chlorination by-products are reduced.

During the last decade, significant advances have been achieved in the synthesis of nanoparticles. The term of nanoparticles is generally used to indicate particles with diameters smaller than 100 nm and materials with at least one dimension in the nanometer scale. Such ultrafine particles fall into transition states between molecular and bulk-sized particles and exhibit unusual physical and chemical properties [3]. Nano-TiO₂ shows high surface area per unit volume, which causes an increase of activity as a catalyst. In the present paper the investigations have been extended to the ozonation of nitrobenzene with nano-TiO₂ as catalyst. This compound was selected as the refractory model pollutant because of its high abundance in industrial wastewater as well as its considerably low reactivity towards biochemical and chemical oxidation.

2. Experimental methods

2.1. Preparation and characterization of catalyst

Nano-TiO₂ used in this study was prepared by the sol–gel method. The yellowish titanium dioxide sol was prepared by mixing tetrabutylorthotitanate and absolute ethanol with a volumetric ratio of 1:4 at room temperature. The sol turned into ivory gel after ageing. Then, the samples were dried and calcined at various temperatures.

* Corresponding author. Tel.: +86 451 86282292; fax: +86 451 82368074.
E-mail addresses: yangyixin@hit.edu.cn, yyx-yy@163.com (Y. Yang),
majun@hit.edu.cn, majun_hit@163.com (J. Ma).

XRD studies of catalyst were performed by means of a D/max-r B diffractometer, at 40 kV, 30 mA (1200 W) and using nickel-filtered Cu α radiation to determine crystal phase and estimate crystallite size. S_{BET} was measured on a ST-2000 nitrogen adsorption equipment (China). TEM was characterized in a JEM-1200 electron microscope (Japan). Zeta potential measurements of TiO₂ were carried out by a Zeta-Meter System JS94G⁺ (China).

2.2. Ozonation procedure

Ozonation tests were conducted in a bench scale system, which consists of a XFZ-581 ozone generator (China), a 1000 mL reactor, and a magnetic stirrer worked with the gas diffuser to achieve a sufficient recirculation of the mixture. Ozone was produced from pure oxygen and fed into the reactor through a porous glass diffuser located at the bottom of the reactor to produce fine bubbles. The residual ozone in the off-gas was adsorbed by KI solution. Concentration of dissolved ozone in water was measured by the Indigo method [4].

The model water was prepared by spiking nitrobenzene in distilled water. The initial concentration of nitrobenzene was about 60 $\mu\text{g L}^{-1}$. Nano-TiO₂ powders were dispersed in the solution as soon as the ozone gas contacted the nitrobenzene solution. Samples were withdrawn at different intervals to determine the residual concentration of nitrobenzene. The oxidation reaction was quenched by the addition of a small amount of sodium thiosulphate. Before measurement, suspensions were filtered with 0.2 μm microfilters to collect the filtrate.

2.3. Analysis

The nitrobenzene concentration was analyzed by using a SP-502 gas chromatograph equipped with an electron capture detector (China). The chromatography conditions were as follows: column temperature: 160 °C; detector temperature: 200 °C; injector temperature: 200 °C; carrier gas: nitrogen.

2.4. Determination of hydroxyl radicals by EPR

EPR experiments were conducted for the determination of hydroxyl radicals generated in solution. A nitron spin-trapping reagent DMPO (5,5-dimethyl-1-pyrrolin-N-oxide), which was purchased from Fluka, was used in the process. DMPO, TiO₂ suspensions were mixed with 500 μL of ozone solution, which was prepared by continued bubbling to water with ozone to obtain an ozone stock solution of 14 mg L^{-1} at 4 °C. Immediately after mixing, the sample solution was transferred into a 100 μL capillary tube which was then fixed in the cavity of the EPR spectrometer. In succession, the EPR spectrum was measured at room temperature with an EPR spectrometer (Bruker EMX-8/2.7 ESR spectrometer with ER 4102ST cavity) under the following experimental conditions: X-field sweep; center field 3480.00 G; sweep width 100.00 G; static field 3490.00 G; frequency 9.751000 GHz; power 4.00 mW. Samples were scanned and accumulated 10 times for 20.972×10 s.

Table 1
XRD results of TiO₂ calcined at different temperatures

Temperature (°C)	Amorphous (%)	Anatase (%)	Rutile (%)	Crystallinity size (nm)
0	100	0	0	5
300	0	100	0	6
400	0	73	27	7
500	0	35	65	20
600	0	6	94	25
700	0	0	100	30

3. Results and discussion

3.1. Effect of calcination temperature

TiO₂ crystallizes in three major different structures: rutile, anatase and brookite. However, only rutile and anatase play important role in the applications of TiO₂ and are of any interest here. Calcination is a common treatment method used to improve the crystallinity of TiO₂ powders. Table 1 shows the XRD results of TiO₂ as synthesized and subsequently calcined at different temperatures from 300 to 700 °C. TiO₂ without calcination is largely amorphous. When TiO₂ powders were calcined at 300 °C, amorphous transformed to anatase completely. As the calcination temperature continued to increase above 400 °C, small rutile peaks in XRD measurement were found, indicating the transformation of anatase to rutile. Finally, the anatase-rutile transformation was complete at the temperature of 700 °C. The approximate crystallite size was estimated by the Scherrer formula, which is generally an accepted method to estimate the mean crystallite size [5].

TEM micrographs of the TiO₂ samples are shown in Fig. 1. The particle size is slightly larger than that formulated by the diffracting angle and line width of corresponding X-ray diffraction peaks. But the TEM results show good consistency with that of XRD. TiO₂ calcined at higher temperature tended to conglomeration in the formation process. Hence, the particle size increased with the increasing calcination temperature, which is contrary to BET surface area, as can be seen in Table 2.

The catalytic efficiency of TiO₂ is strongly related to the crystal structure and the surface morphology. It has been reported that anatase is more active in many photocatalytic processes [6–8]. But not any report has been found about the catalytic ozonation process. Fig. 2 represents the relationship between the calcination temperature and catalytic

Table 2
BET of TiO₂ calcined at different temperatures

Temperature (°C)	BET (m ² /g)
0	224.43
300	113.81
400	81.79
500	40.13
600	11.59
700	3.04

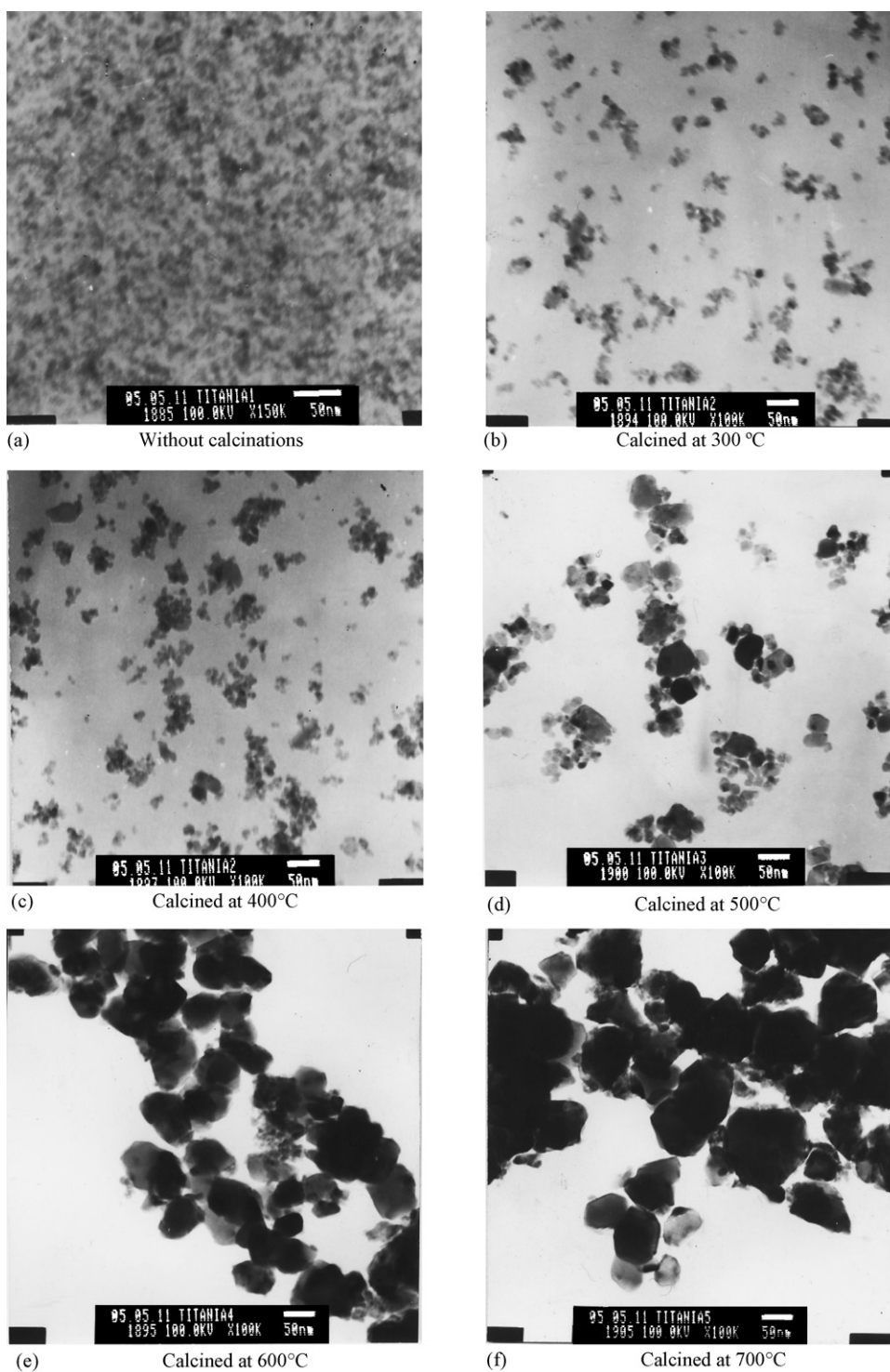


Fig. 1. TEM micrographs of TiO_2 calcined at different temperatures: (a) without calcinations; (b) calcined at 300 °C; (c) calcined at 400 °C; (d) calcined at 500 °C; (e) calcined at 600 °C; (f) calcined at 700 °C.

activity of the prepared TiO_2 . Amorphous TiO_2 catalyzed ozonation caused significant nitrobenzene abatement, but the processes of calcination at 300–400 °C induced a decrease of the removal efficiency of nitrobenzene, and the calcination of TiO_2 at 500–700 °C achieved some elevation of catalytic activity. Rutile is the main component of TiO_2 calcined at 500–700 °C. That is to say, differing from photocatalysis, amorphous and

rutile are more competent for catalytic ozonation than anatase. Because TiO_2 calcined at 500 °C showed the best catalytic activity, it was adopted for the latter research. In the presence of TiO_2 calcined at 500 °C, about 55% of nitrobenzene in the solution could be ozonated. It is evident that nano- TiO_2 catalyzed ozonation presents a high potential to destroy nitrobenzene.

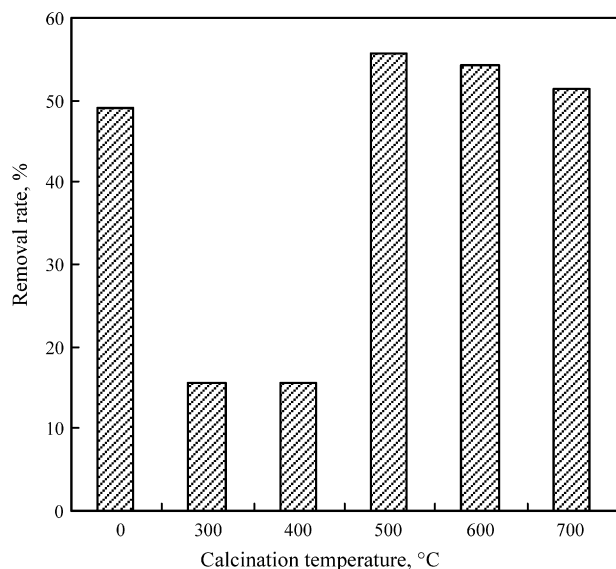


Fig. 2. Variation of the catalytic activity as a function of calcination temperature of TiO_2 (ozone applied $0.367 \pm 0.02 \text{ mg L}^{-1}$, TiO_2 0.1 g L^{-1} , NB $60 \mu\text{g L}^{-1}$, reaction time 20 min, temperature 20°C).

3.2. Effect of catalyst dose

Effect of catalyst dose on the degradation of nitrobenzene is shown in Fig. 3. It is observed that ozonation of nitrobenzene was rather limited at ambient temperature in the absence of TiO_2 catalyst. Since the direct reaction of nitrobenzene with ozone is very slow ($k = 0.09 \pm 0.02 \text{ L mol}^{-1} \text{ s}^{-1}$) [9] then it seems reason-

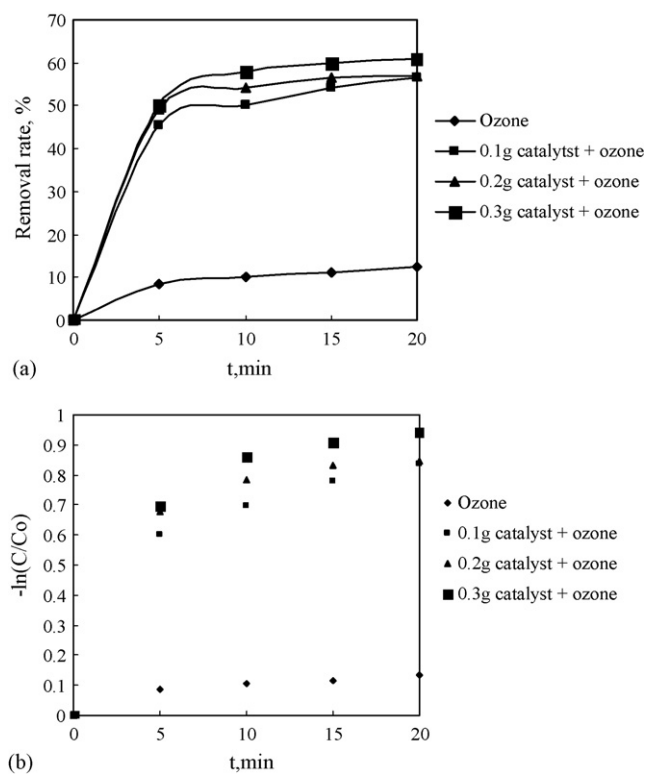


Fig. 3. Catalytic ozonation of nitrobenzene with different catalyst mass (ozone applied $0.367 \pm 0.02 \text{ mg L}^{-1}$, NB $60 \mu\text{g L}^{-1}$, temperature 20°C): (a) effect of catalyst dose and (b) kinetic study of different catalyst dose.

able to admit that the poor conversion of nitrobenzene achieved in the non-catalytic ozonation process was due to the action of free radicals generated from self-decomposition of ozone. It is well known that ozonation of blank water also results in the production of hydroxyl radicals through ozone decomposition [10]. The reaction rate constant of hydroxyl radicals with nitrobenzene can reach $3.9 \times 10^9 \text{ L mol}^{-1} \text{ s}^{-1}$ [9]. These radicals are supposed to be responsible for the degradation of nitrobenzene in the process of ozonation alone, which was verified in the later EPR experiments.

The removal efficiency of nitrobenzene was significantly improved at the presence of both ozone and catalyst. A unique property of nanoparticles is their extremely high surface area. As can be found from experiments, adsorption of nitrobenzene on TiO_2 can cause approximate 30% disappearance of this compound at a catalyst loading of 0.1 g L^{-1} . Thus, the nitrobenzene removal rate of the simultaneous application of ozone and TiO_2 was higher than the sum of the individual contributions of single ozonation and single adsorption. It is evident that removal of nitrobenzene was due to the action of some ozone absorbed species or free radicals generated probably on the catalyst surface or in the aqueous bulk.

Catalyst dose exerted a positive influence on nitrobenzene conversion in catalytic ozonation process. But the increase of catalyst dose did not yield any significant increase of the oxidation rate as illustrated in Fig. 3a. Nitrobenzene in water degraded rapidly within the first 5 min, and then the reaction rate became slower. Since ozone gas was discontinuously generated in the experimental system, a slightly higher ozone concentration will be present in the reactor for the first few minutes, which results in a faster initial reaction rate. It is shown in Fig. 3b that conversion of nitrobenzene followed pseudo-first-order kinetic equation after the first 5 min during ozonation and catalytic ozonation.

3.3. Effect of initial concentration of nitrobenzene

Figs. 4 and 5 present the effect of initial concentration of nitrobenzene on the adsorption and catalytic ozonation processes, respectively. As shown in Fig. 4a, increasing uptake on increasing nitrobenzene concentration is initially observed but with the saturation of the extent of adsorption at higher nitrobenzene concentrations. This adsorption data is adequately described by a Langmuir isotherm expression:

$$S_{\text{NB}} = \frac{KL_{\text{NB}}S_{\text{NB,max}}}{1 + KL_{\text{NB}}} \quad (1)$$

where L_{NB} and S_{NB} are the concentration of nitrobenzene in solution and on the solid, respectively after 20 min contact with the solid; K is the conditional equilibrium constant (for formation of an adsorbed nitrobenzene species); and $S_{\text{NB,max}}$ represents the maximum concentration of nitrobenzene that may be adsorbed to the TiO_2 surface (within the 20 min equilibration time allowed). Linear transformation of Eq. (1) yields an expression of the form:

$$\frac{L_{\text{NB}}}{S_{\text{NB}}} = \frac{1}{S_{\text{NB,max}}}L_{\text{NB}} + \frac{1}{KS_{\text{NB,max}}} \quad (2)$$

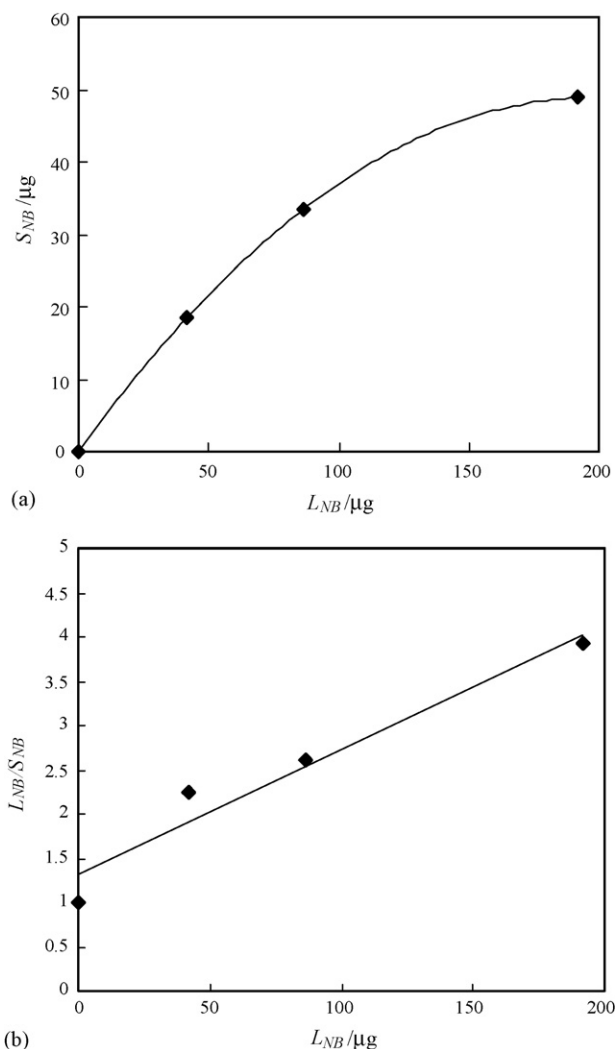


Fig. 4. Adsorption curve of nitrobenzene on TiO_2 (TiO_2 0.1 g L^{-1} , adsorption time 20 min, temperature 20°C): (a) concentration of NB adsorbed as a function of the solution concentration and (b) the rectangular hyperbola of best fit as determined by linear transformation.

which, when fitted to the available data (Fig. 4b), provides an estimate for $S_{\text{NB,max}}$ of $87.72 \mu\text{g}$ at neutral pH. Given that 0.1 g L^{-1} TiO_2 has been used in these adsorption studies, this represents a maximum adsorption density of $877.2 \mu\text{g}$ of nitrobenzene per gram of TiO_2 at neutral pH.

Catalytic ozonation was accelerated by increasing the initial concentration of nitrobenzene as can be seen from Fig. 5. And the degradation of nitrobenzene can also be divided into two stages. There was a rapid initial reaction rate in the initial 5 min of contact time, and then the reaction followed pseudo-first-order kinetic equation after the first 5 min. Effect of initial nitrobenzene on initial reaction rate and the second stage reaction rate are presented in Fig. 6. It is concluded that the reaction rate of the first 5 min was in direct proportion to the initial nitrobenzene concentration. And the first-order reaction rate of the second stage was also related to the initial concentration of nitrobenzene.

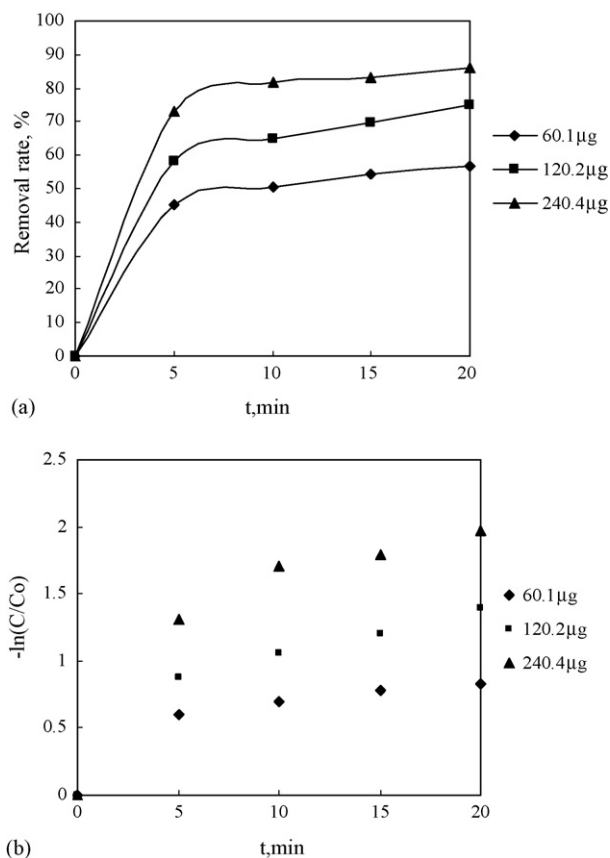
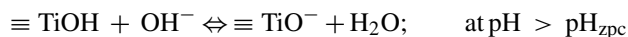


Fig. 5. Effect of initial nitrobenzene on catalytic ozonation (ozone applied $0.367 \pm 0.02 \text{ mg L}^{-1}$, TiO_2 0.1 g L^{-1} , temperature 20°C): (a) effect of different initial NB concentration and (b) kinetic study of different initial NB concentration.

3.4. Effect of pH

Since pH is a key parameter for both ozone stability and catalyst surface properties in aqueous solution, it is important to examine the influence of pH on catalytic ozonation. As shown in Fig. 7, all processes seem to be pH sensitive in the range 2–10.

Adsorption of nitrobenzene on TiO_2 varies largely with the pH of solution, a fact that can be assigned to the strong dependence of catalyst surface phenomena on pH. It is well established that upon hydration, the TiO_2 surface develops hydroxyl groups, which can undergo a proton association or dissociation reaction:



where $\equiv \text{TiOH}_2^+$, $\equiv \text{TiOH}$ and $\equiv \text{TiO}^-$ are positive, neutral and negative hydrous TiO_2 surface functional groups, respectively. In very simple terms, interactions with cationic electron donors and electron acceptors will be favored for heterogeneous chemisorption at high pH under conditions in which $\text{pH} > \text{pH}_{\text{zpc}}$, while anionic electron donors and acceptors will be favored at low pH under conditions in which $\text{pH} < \text{pH}_{\text{zpc}}$ [11].

Since nitrobenzene is a kind of unionizable compound, the adsorption density is consistent with the concentration of the surface sites $\equiv \text{TiOH}$ that can support the adsorption of nitroben-

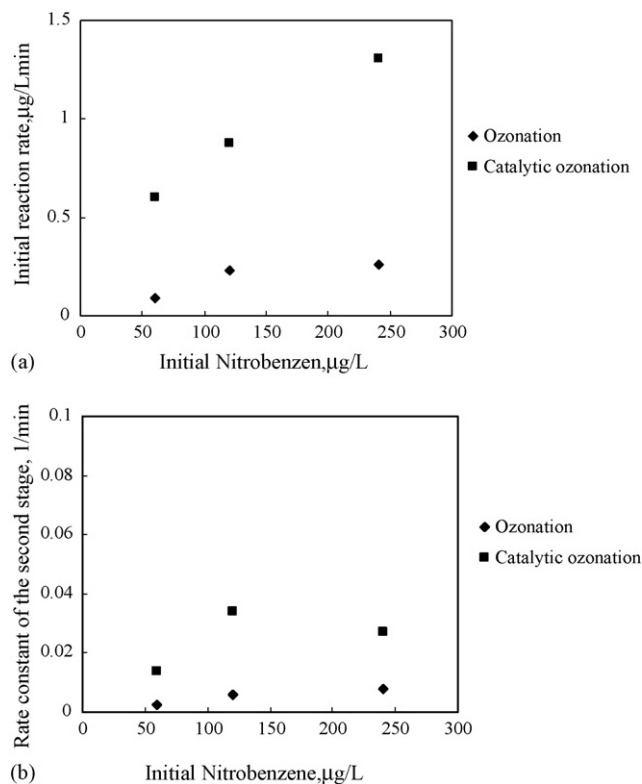


Fig. 6. Effect of initial nitrobenzene concentration on reaction rate (ozone applied $0.367 \pm 0.02 \text{ mg L}^{-1}$, TiO_2 0.1 g L^{-1} , reaction time 20 min, temperature 20°C): (a) effect of initial NB on the reaction rate in the first 5 min and (b) effect of initial NB on the first-order reaction rate in the second stage.

zene. It implies that nitrobenzene will be adsorbed by the greatest extent on catalyst surface under conditions in which $\text{pH} = \text{pH}_{\text{zpc}}$. In determining the pH_{zpc} (point of zero charge) of TiO_2 , 0.1 g of TiO_2 powder was dispersed in 1 L re-distilled water, the initial pH was measured and recorded. The solution pH was then adjusted with HCl or NaOH to cover a range from pH 3 to 11. Zeta potential measurements showed that the pH_{zpc} of TiO_2 is 6.4. Thus, the pH of maximum adsorption density is around 6.4, which keep consistent with the experimental results.

It is well known that ozone decomposes into hydroxyl radicals more easily in basic solution than neutral or acid cir-

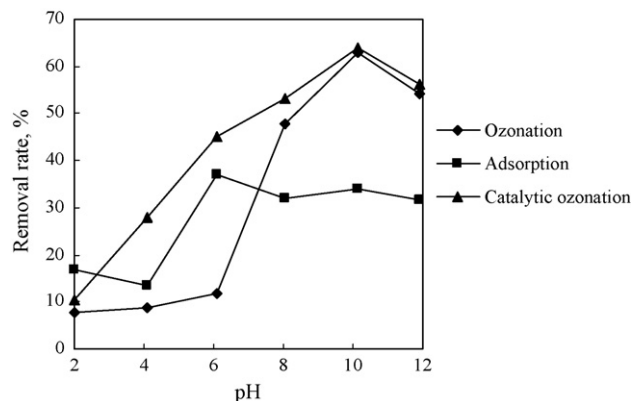


Fig. 7. Influence of pH on the degradation of nitrobenzene (ozone applied $0.367 \pm 0.02 \text{ mg L}^{-1}$, TiO_2 0.1 g L^{-1} , reaction time 20 min, temperature 20°C).

cumstances because hydroxide ions may play a role of initiator of the chain reaction [12]. Hence, more nitrobenzene molecules can be oxidized in a basic pH solution since the concentration of hydroxyl radicals is much higher than acid solution. From Fig. 10, it can be seen that the removal rate of ozonation was especially low at pH 2 and increased with the increase of pH value. Significantly, the pH dependence of the nitrobenzene removal rate of ozonation was approximately reflected by the extent of removal rate of catalytic ozonation as a function of pH. Hardly any increase of the removal rate was obtained for catalytic ozonation compared to ozonation alone when pH was above 10. This fact may be explained as that oxidation with ozone was already strong under an alkaline environment.

It runs in a parallel relationship between pH and removal efficiency for ozonation and catalytic ozonation. This indicates that both ozonation and catalytic ozonation are likely to follow a similar mechanism. However, it is probably the coupling of the heterogeneous initiation followed by the homogeneous promotion of the ozone decomposition reaction, which accounts for the observed effects. It is assumed that the initiating chain reactions happening in the solution are very important for the whole catalytic ozonation process. That is to say, hydroxyl radicals stand a great chance of generating mainly in the water phase rather than on the catalyst surface. The confirmation to these assumptions will need much further study to be fully elucidated and as such is beyond the scope of this study.

3.5. Mechanism of TiO_2 catalyzed ozonation

One of proposed catalytic mechanisms assumes that the catalyst performs double function. Its presence causes both an increase of ozone dissolution and the initiation of ozone decomposition reaction [13]. Because of the interferences of suspending TiO_2 powders, dissolved ozone concentration could not be determined instantly. Hence, we cannot directly figure out how TiO_2 act in the radical chain reaction. Indirect evaluation was made by examining the effect of radical scavengers.

Experiments were carried out in the presence of *tert*-butyl alcohol and carbonate as radical scavengers. Species like OOCH_2COO and CO_3^{2-} can also react with the hydroxyl radicals produced. These reactions form secondary radicals, which do not predominantly produce the HO_2^\bullet and $^\bullet\text{O}_2^-$ radicals, then result in the termination of chain reactions. *tert*-butyl alcohol is a relatively stronger radical scavenger than carbonate due to its higher reaction rate constant with hydroxyl radicals ($K_{\text{tert-butyl alcohol}} = 5 \times 10^8 \text{ L mol}^{-1} \text{ S}^{-1}$, $K_{\text{Carbonate}} = 3.9 \times 10^8 \text{ L mol}^{-1} \text{ S}^{-1}$) [14]. And the influence of *tert*-butyl alcohol is highly greater than carbonate as illustrated in Figs. 8 and 9.

It can be seen that the presence of *tert*-butyl alcohol significantly decreased the nitrobenzene removal rate of ozonation and catalytic ozonation, which keep consistent with the free radical characteristics. The presence of *tert*-butyl alcohol at a concentration of 2 mg L^{-1} in water caused a reduction of 30% in the removal rate of catalytic ozonation. There was still a part of nitrobenzene removed from water, which can be contributed to the adsorption effect of the catalyst. Neither *tert*-butyl

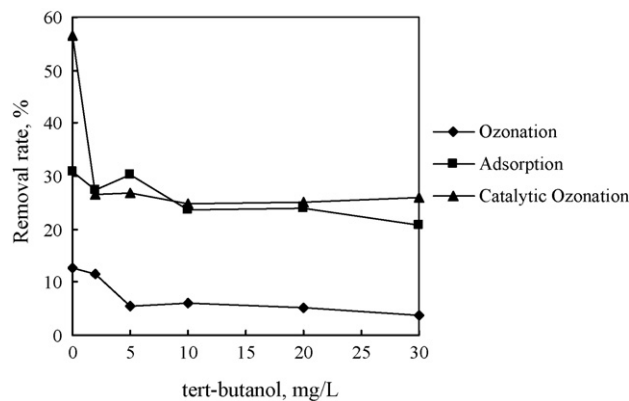


Fig. 8. Effect of *tert*-butyl alcohol on the degradation of nitrobenzene (ozone applied $0.367 \pm 0.02 \text{ mg L}^{-1}$, TiO_2 0.1 g L^{-1} , reaction time 20 min, temperature 20°C).

alcohol nor carbonate caused any great influence on the adsorption of nitrobenzene on catalyst. However, the removal rate of nitrobenzene did not decrease any more when keep on increasing the concentration of *tert*-butyl alcohol. Carbonate had less scavenging effect than *tert*-butyl alcohol. An interesting fact was found that the efficiency of ozonation and catalytic ozonation actually increased in the presence of a small amount of carbonate (10 mg L^{-1}). These results suggest that low concentration of carbonate plays a role as promoter during ozone decomposition. While at higher concentrations of carbonate, the radical-scavenging effect can be observed, which proved the free radical mechanism also.

However, it is very important to directly identify whether hydroxyl radicals is generated in TiO_2 catalyzed ozonation process. Since hydroxyl radicals are a kind of short-lived species, it is difficult to hold and then measure it like other stable substances. Electron spin resonance (EPR) enables the detection of radicals, and the spin-trapping/EPR technique has been developed to detect unstable radicals [15]. Unstable free radicals are converted to the corresponding stable spin-adducts by binding spin-trapping reagents, and the spin-adducts are measured by EPR spectroscopy. The pattern of the resulting EPR spectrum is strongly changed by the free radicals bound, and then the kind as well as the amount of free radicals can be determined

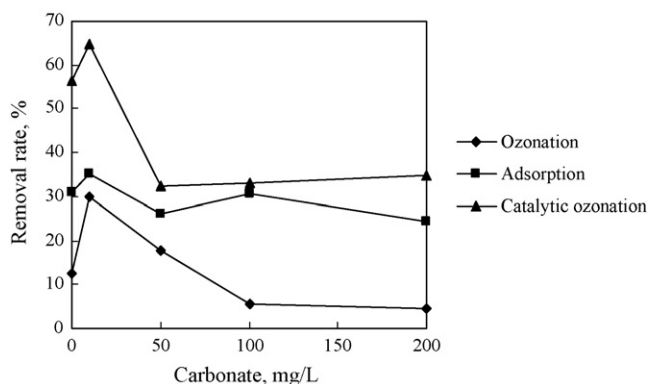


Fig. 9. Effect of carbonate on the degradation of nitrobenzene (ozone applied $0.367 \pm 0.02 \text{ mg L}^{-1}$, TiO_2 0.1 g L^{-1} , reaction time 20 min, temperature 20°C).

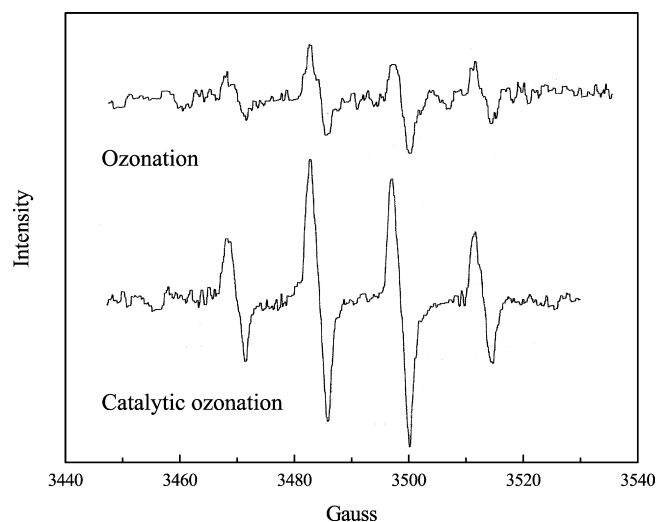


Fig. 10. Comparison of the intensity of DMPO-OH adducts signals of ozonation and catalytic ozonation (DMPO 100 mmol , O_3 6 mg L^{-1} , TiO_2 600 mg L^{-1}).

from the EPR parameter and its signal intensity. This technique has been applied to the investigation of hydroxyl radicals generated in water during ozonation (Utsumi H, 1994) and ultrasonic irradiation process [16].

For the confirmation of mechanism mentioned above, spin trapping/EPR technique was applied for measuring the hydroxyl radicals generated in ozonation and TiO_2 -catalyzed ozonation. Fig. 10 showed the typical EPR spectrum obtained during ozonation and catalytic ozonation. The spectrum was composed of quartet lines having a peak height ratio of 1:2:2:1 and the parameters were hyperfine constants $\alpha_N = 1.49 \text{ mT}$, $\alpha_H = 1.49 \text{ mT}$ and $g\text{-value} = 2.0055$. These parameters coincided with those of the DMPO-OH adduct as demonstrated previously [17]. It can be found that the signals observed in catalytic ozonation were stronger than that in ozonation alone. Namely, it is verified that the presence of TiO_2 powders accelerated the generation of hydroxyl radicals in the ozonation system.

As reported by Nawrocki [18], hydroxyl groups are present on TiO_2 surface in water. It is supposed that these hydroxyl groups react with dissolved ozone to generate unstable species, which can act as the promoter of chain reactions to produce hydroxyl radicals. Based on the analysis of experimental data, hydroxyl radicals are generated mainly in solution. Although it is short of fundamental study, great surface area possessed by nanoparticles is considered as one reason of catalytic activity for TiO_2 . Further research is now in progress and will be discussed in another paper.

4. Conclusions

Use of nano- TiO_2 powder as catalyst for the ozonation of nitrobenzene in water significantly improved the removal of this compound compared with ozonation alone. Rutile showed better catalytic activity than anatase. An increase of initial nitrobenzene concentration caused the enhancement of nitrobenzene removal by ozonation and catalytic ozonation. Whereas, increasing the dose of catalyst showed negligible influence on

nitrobenzene removal. The removal rate increased with increasing pH of solution for catalytic ozonation. The presence of either *tert*-butyl alcohol or carbonates had a negative effect on catalytic ozonation. These experimental results confirmed the proposition that the degradation of nitrobenzene by TiO₂-catalyzed ozonation followed a radical-type mechanism. Moreover, the EPR experiments verified that the production of hydroxyl radicals was accelerated by the addition of TiO₂, which consequently resulted in the enhancement of nitrobenzene removal rate.

Acknowledgement

Support from the National Natural Science Foundation of China (No. 50578051) is greatly appreciated and acknowledged.

References

- [1] H. Paillard, M. Doréand, M.M. Bourbigot, Proceedings of the 10th World Congress of the International Ozone Association, Mónaco, 1991.
- [2] R. Gracia, S. Cortes, Proceedings of the 13th World Congress of the International Ozone Association, Kyoto, Japan, 1997.
- [3] N. Suddhasattwa, S. Parvesh, J. Colloid Interface Sci. 264 (2003) 89–94.
- [4] H. Bader, J. Hoigné, Water Res. 15 (1981) 449–456.
- [5] B.D. Cullity, Elements of X-Ray Diffraction, Adison-Wesley, London, 1978.
- [6] R.J. Berry, M.R. Mueller, Microchem. J. 50 (1994) 28–32.
- [7] M.R. Hoffman, S.T. Martin, Chem. Rev. 95 (1995) 69–96.
- [8] W. Ma, Z. Lu, Appl. Phys. A Mater. Sci. Process. 66 (1998) 621–627.
- [9] J. Hoigné, H. Bader, Water Res. 17 (1983) 173–183.
- [10] J. Staechlin, J. Hoigné, Environ. Sci. Technol. 19 (1985) 1208–1213.
- [11] L. Ming-Chun, R. Gwo-Dong, Water Res. 30 (1996) 1670–1676.
- [12] J. Staechlin, J. Hoigné, Environ. Sci. Technol. 16 (1982) 676–681.
- [13] C. Cooper, R. Burch, Water Res. 33 (1999) 3695–3700.
- [14] J.L. Acero, V. Gunten, Proceedings of Ozonation and AOPs in Water Treatment: Applications and Research, France, 1998.
- [15] E.G. Janzen, B.J. Blackburn, J. Am. Chem. Soc. 91 (1969) 4481–4490.
- [16] S.K. Han, S.N. Nam, Water Sci. Technol. 46 (2002) 7–12.
- [17] H. Utsumi, M. Hakoda, Water Sci. Technol. 30 (1994) 91–99.
- [18] J. Nawrocki, M.P. Rigney, J. Chromatogr. A. 657 (1993) 229–282.